THE JOURNAL OF PHYSICAL CHEMISTRY Letters

pubs.acs.org/JPCL Letter

Direct Growth of Continuous and Uniform MoS_2 Film on SiO_2/Si Substrate Catalyzed by Sodium Sulfate

Guanmeng Li, Xiaoli Wang, Bo Han, Weifeng Zhang, Shuyan Qi, Yan Zhang, Jiakang Qiu, Peng Gao, Shaoshi Guo, Run Long, Zhenquan Tan,* Xue-Zhi Song,* and Nan Liu*

Cite This: J. Phys. Chem. Lett. 2020, 11, 1570−1577 Read Online

ACCESS | Metrics & More | Article Recommendations | Supporting Information

ABSTRACT: Because of its unique electronic band structure, molybdenum disulfide (MoS_2) has been regarded as a star semiconducting material. However, direct growth of continuous and high-quality MoS_2 films on SiO_2/Si substrates is still very challenging. Here, we report a facile chemical vapor deposition (CVD) method based on synergistic modulation of precursor and Na_2SO_4 catalysis, realizing the centimeter scale growth of a continuous MoS_2 film on SiO_2/Si substrates. The as-grown MoS_2 film had an excellent spatial homogeneity and crystal quality, with an edge length of the composite domain as large as 632 μm. Both experimental and theoretical results proved that Na tended to bond with SiO_2 substrates rather than to interfere with as-grown MoS_2. Thus, they showed decent and uniform electrical performance, with electron mobilities as high as 5.9 $cm^2\ V^{-1}\ s^{-1}$. We believe our method will pave a new way for MoS_2 toward real application in modern electronics.

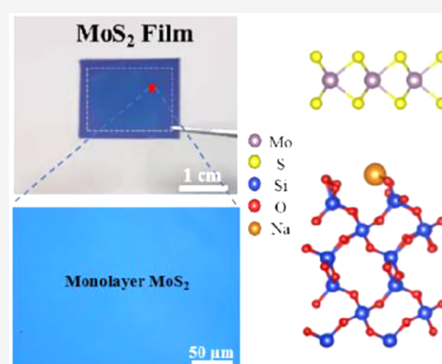

Downloaded via ZHEJIANG UNIV on September 5, 2023 at 02:42:50 (UTC).
See https://pubs.acs.org/sharingguidelines for options on how to legitimately share published articles.

Two-dimensional layered transition-metal dichalcogenide (TMD) materials have been widely explored as the most promising replacements for Si,[1−3] and molybdenum disulfide (MoS_2) with a band gap of 1.2−1.9 eV and a thickness scaling feature is a representative example.[4−7] MoS_2 has unique electrical and optoelectrical properties, including high light absorption, large excitonic effect, band gap modulation, strong piezoelectricity, and so on. It has wide prospective uses in the applications of well-controlled electrostatics in ultrashort transistors,[8,9] ultrasensitive optoelectrical devices,[10,11] and piezoelectrical sensors.[12] The prerequisite of all the above-mentioned advanced electronic and optoelectronic applications is large-scale growth of high-quality and continuous MoS_2 thin films. Thus, developing a reliable and scalable synthetic method for MoS_2 film is highly desired.[13−16]

Researchers have devoted extensive efforts to growing large-area and continuous MoS_2 films, such as conventional chemical vapor deposition,[17] metal−organic chemical vapor deposition (MOCVD),[18−20] physical vapor deposition (PVD),[21,22] atomic layer deposition (ALD),[23] and thermal deposition.[24,25] Among them, MOCVD is able to achieve high-quality MoS_2 films with average electron mobility of 30 $cm^2\ V^{-1}\ s^{-1}$ at room temperature. However, it requires very expensive equipment and may introduce carbon-based contaminations from organic compounds during the reaction, where device performance may deteriorate.[14] Although PVD and ALD are less expensive than MOCVD, they can achieve only low-quality MoS_2 films with very small grain size and low carrier mobility, which cannot be used for real applications in high-speed electronic devices. Conventional CVD growth of MoS_2 films is most widely explored because of its low cost as well as scalable production. To improve the crystallinity of MoS_2 films, hydrogen,[26] oxygen, or other harsh conditions are specifically introduced,[15,18] but they may lead to potential safety hazards in practical applications. For example, Yang et al. successfully synthesized uniform monolayer MoS_2 film with large domain size on solid soda-lime glass by introducing a rush of O_2.[15] Recently, it has been observed that the addition of selected synergistic additives to the CVD substrates, such as alkali metal halides,[27−31] KOH,[32] fluorides,[33] and seed catalysts can result in exponential increase of growth area for 2D materials.[34,35] Liu's group reported that NaCl-mediated CVD can be widely used in the synthesis of various 2D TMDs and accomplish the growth of millimeter-scale MoS_2 single crystal.[28] However, all the above catalyst-mediated growth of continuous MoS_2 films happen on sapphire, mica, and glass,[31,36] which are not compatible with Si-based technology. Therefore, there still remains a big challenge in attaining MoS_2 film being large-area, continuous and high-quality at the same time, in particular directly on SiO_2/Si substrates.

Herein, we report a precursor and catalyst co-mediated method for fabrication of centimeter-scale, continuous, and high-quality MoS_2 films directly on SiO_2/Si substrates. This method demonstrated the growth of a large-area MoS_2 film

Received: December 29, 2019
Accepted: February 3, 2020
Published: February 3, 2020

ACS Publications © 2020 American Chemical Society

https://dx.doi.org/10.1021/acs.jpclett.9b03879
J. Phys. Chem. Lett. 2020, 11, 1570−1577

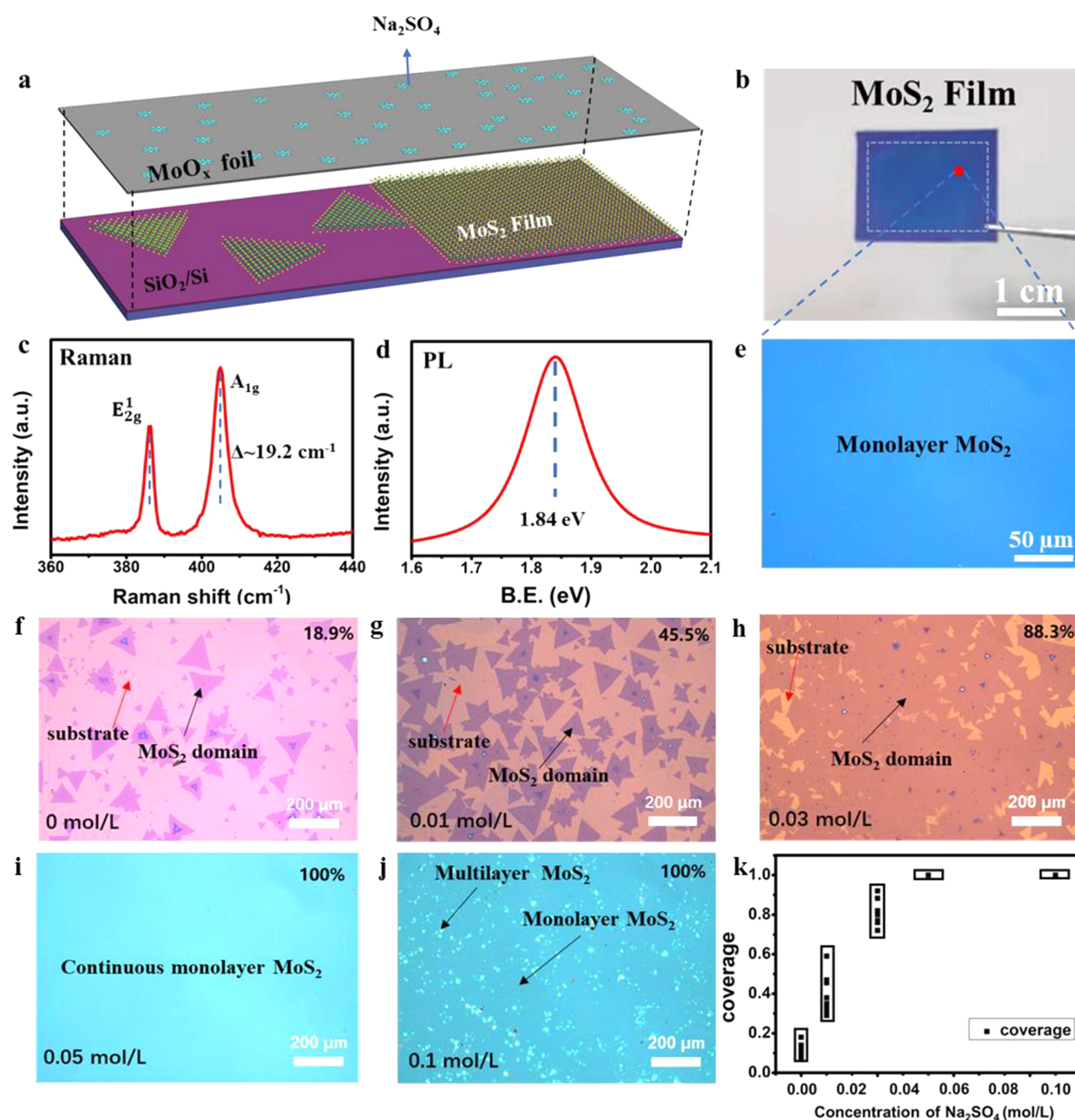

Figure 1. Centimeter-scale growth of MoS_2 film. (a) Schematic diagram of face-to-face growth of MoS_2 film. Top: MoO_x foil as precursor and Na_2SO_4 as catalysts. Bottom: as-grown MoS_2 film on SiO_2/Si substrate. (b) Photograph of centimeter-scale MoS_2 film on SiO_2/Si promoted by 0.05 mol/L Na_2SO_4. (c and d) Raman and photoluminescence spectra of as-grown monolayer MoS_2 in panel b. (e) Optical image of uniform and continuous MoS_2 film taken from panel b. (f) Optical image of sporadic MoS_2 domains on SiO_2/Si substrate without the promotion of Na_2SO_4. (g−j) Optical images of MoS_2 domains/films on SiO_2/Si substrate with the promotion of Na_2SO_4 (0.01, 0.03, 0.05, and 0.1 mol/L). (k) Statistical chart of coverage of MoS_2 as a function of Na_2SO_4 concentration.

with the composite domains possessing an edge length as large as 632 μm on the SiO_2/Si substrate. This immediately allowed us to fabricate FET arrays with standard photolithography rather than relying on complicated electron beam lithography (EBL) to selectively design contact electrodes on randomly small domains. They showed a maximum carrier mobility of 5.9 $cm^2\ V^{-1}\ s^{-1}$ and an on/off current ratio of $\sim 10^5 - 10^6$ at room temperature, which was comparable to those grown by many methods.[15,24,25,29] We propose a synergistic mechanism in which precursor regulation and Na_2SO_4 catalysis co-contributed to large-area growth of MoS_2 film. The introduction of MoO_x foil as precursor provided a face-to-face growth fashion as well as higher reactive activity than Mo foil. When using Na_2SO_4 as a synergetic additive, not only did the overall reaction rate increase, but also Na atoms tended to bond with SiO_2 substrates rather than to interfere with as-grown MoS_2 based on density functional theory (DFT) calculation and X-ray photoelectron spectroscopy (XPS) study, resulting in high-quality MoS_2 film. This work paves the way to the batch production of high-uniformity and -quality MoS_2 films, which will advance its practical applications in various fields.

Figure 1a schematically illustrates our face-to-face growth process, in which MoO_x foil with the Na_2SO_4 synergistic additive is placed on top of the SiO_2/Si substrate. MoO_x foil with higher chemical activity was chosen as precursor. Na_2SO_4 as synergistic additive was uniformly distributed throughout the foil. The whole reaction was conducted with argon as the only carrier gas without introducing flammable and explosive gases such as hydrogen and oxygen, which ensures the security of large-scale production (see details in Experimental Methods and Figure S1 in the Supporting Information). Figure 1b shows a representative result of the as-grown MoS_2 film on the SiO_2/Si substrate circled by a white dashed line. The film was

https://dx.doi.org/10.1021/acs.jpclett.9b03879
J. Phys. Chem. Lett. 2020, 11, 1570−1577

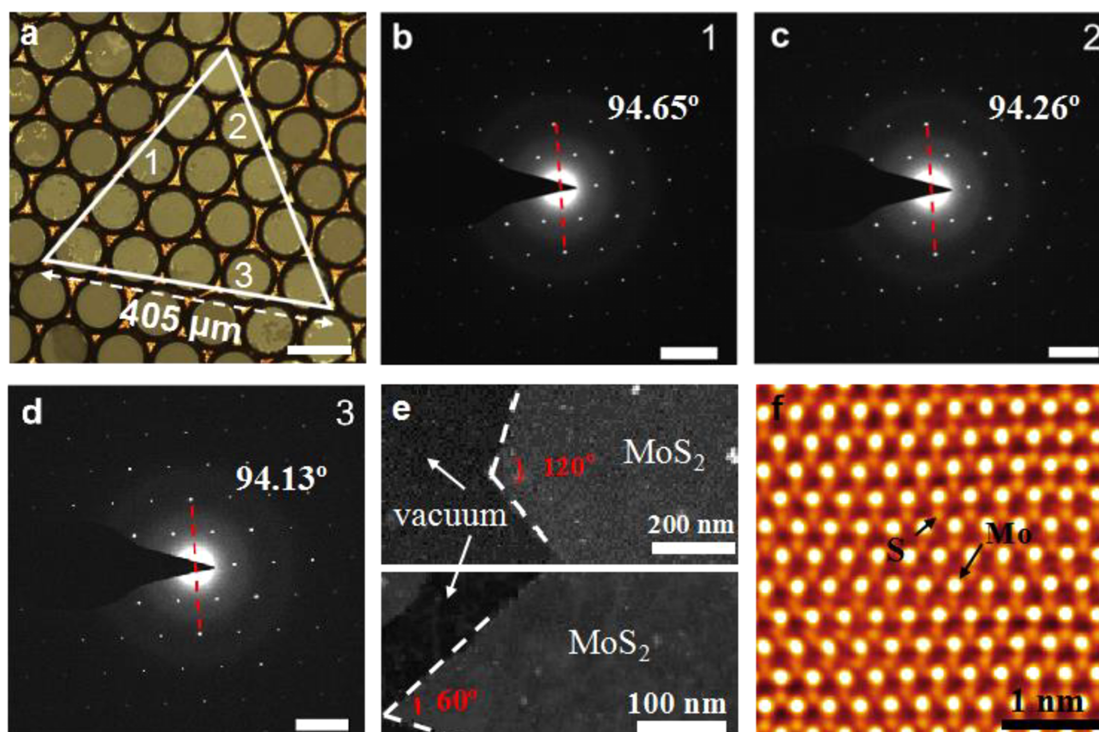

Figure 2. Atomically resolved TEM measurements of MoS_2. (a) Optical image of MoS_2 transferred onto a TEM grid (scale bar: 100 μm). (b−d) SAED patterns from the regions numbered 1−3 in panel a. The dashed lines indicate the rotation angles (94.65°, 94.26°, 94.13°) with respect to the horizontal line (scale bar: 5 nm^{-1}). (e) STEM image of monolayer MoS_2 edge ended with specific edge angles (60° or 120°). (f) Inverse FFT image of monolayer MoS_2. The bright and dim spots correspond to Mo and S atoms, respectively.

centimeter-scale and could be further scalable by increasing the size of the growth chamber. From its magnified optical microscopy (OM) image, a highly uniform color contrast was clearly seen, indicating the uniform thickness and in-plane continuity of the MoS_2 film (Figure 1e). The large MoS_2 crystal domain could be distinguished with an edge length as large as 632 μm encircled by a number of hexagonal contour traces of epitaxial growth (Figure S2a). Then, the layer number and crystal quality of the MoS_2 film were evaluated by Raman and photoluminescence (PL) spectra. The main Raman modes of E^1_{2g} and A_{1g} were observed at ~386.1 and ~405.3 cm^{-1}, corresponding to the intralayer vibrations along the in-plane or out-of-plane directions, respectively, with peak frequency difference of ~19.2 cm^{-1}. The small peak frequency difference is evidence of monolayer MoS_2 (Figure 1c).[37] In the PL spectrum (Figure 1d), the presence of a sharp peak positioned at 1.84 eV with high intensity further revealed the MoS_2 monolayer was of high quality.[26]

In order to investigate the effect of Na_2SO_4 additive on the growth result, different concentrations of Na_2SO_4 were applied on MoO_x foil (Figure 1f−j). Without the Na_2SO_4 additive, sporadic MoS_2 domains were observed on the SiO_2/Si surface. With the concentration of Na_2SO_4 increased, MoS_2 domain size significantly increased. At the concentration of 0.05 mol/L, MoS_2 domains stitched into one film and almost fully covered the SiO_2/Si surface. When the concentration of Na_2SO_4 further increased (c = 0.1 mol/L), multilayer MoS_2 began to appear, indicating a turning point from island growth mode to layer-by-layer mode (Figures 1j and S2b). Thus, in our specific growth environment, 0.05 mol/L Na_2SO_4 was an optimal concentration to achieve uniform and continuous monolayer MoS_2 film. The disappearance of nucleating points at this concentration of Na_2SO_4 was due to the balance of growth rate and mass flux of metal precursor.[28] Statistical analysis of coverage of MoS_2 as a function of Na_2SO_4 concentration also proved that Na_2SO_4 was indeed a promoter on the growth of MoS_2 in terms of growth rate and film coverage (Figure 1k).

Transmission electron microscopy (TEM) and scanning transmission electron microscopy (STEM) were used to probe the microstructure of the continuous MoS_2 film. Figure 2a is an optical image of a typical triangular MoS_2 domain with an edge length of ~405 μm on a TEM grid. We carried out a series of selective area electron diffraction (SAED) measurements on different locations to identify whether the domain is a single crystal (Figure 2a−d). All of the diffraction spots showed strong hexagonal patterns with almost identical lattice orientations (deviation smaller than ±0.52°) (Figure 2b−d), suggesting the single-crystal nature and uniformity across a large area. We also performed atomic-resolution observation by high-angle annular dark field scanning transmission electron microscopy (HAADF-STEM) equipped with aberration-corrected TEM. Over the imaging areas of Figures 2e and S3a−c, MoS_2 was uniform and tended to end with specific edge angles (60° or 120°). It was clearly distinguished that Mo and S atoms were arranged in hexagonal symmetry as highlighted by bright and dim balls in the STEM image and corresponding filtered image using inverse fast Fourier transform (FFT) (Figures S3d and 2f), consistent with the micro-characteristics of MoS_2. Overall, on the basis of the atomic-resolution TEM study, we concluded that the as-grown MoS_2 film is of high uniformity and crystallinity at the atomic scale.

Uniformity of the thin film is an important evaluation criterion in the semiconductor industry. To ensure structural

https://dx.doi.org/10.1021/acs.jpclett.9b03879
J. Phys. Chem. Lett. 2020, 11, 1570−1577

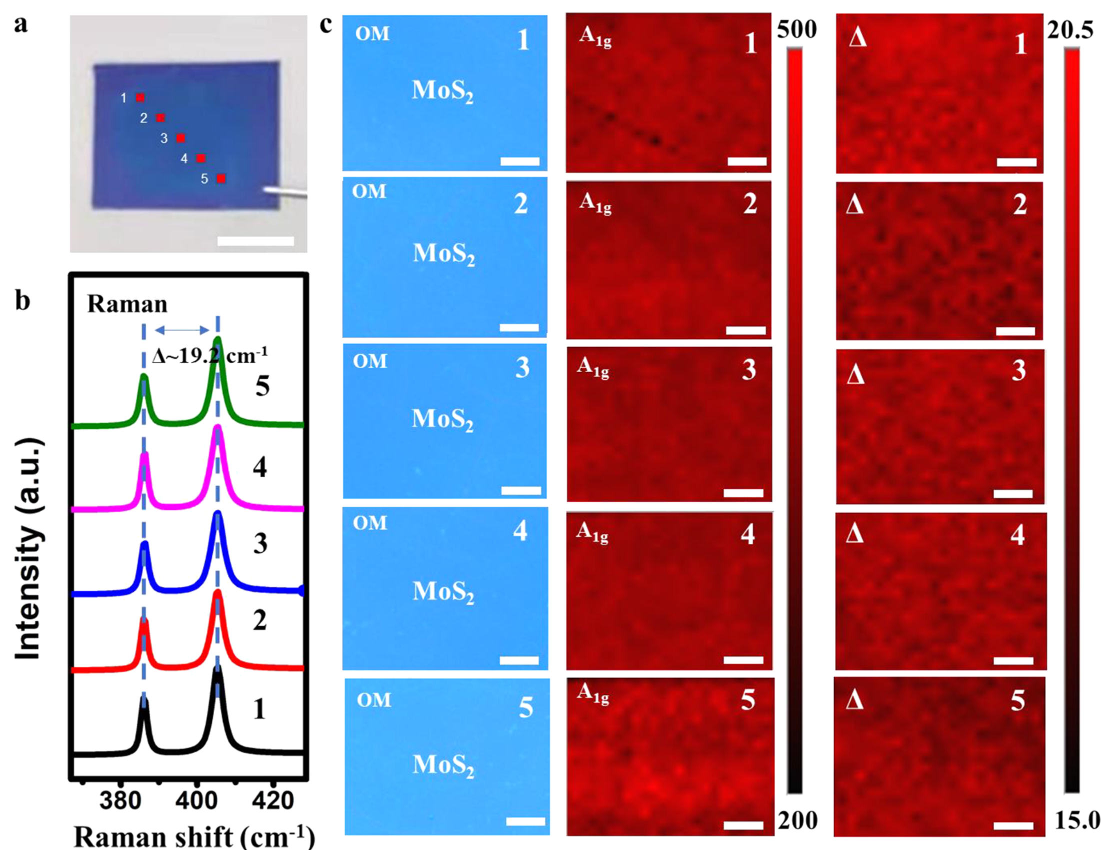

Figure 3. Uniformity of the centimeter-scale MoS_2 film. (a) Photograph of as-grown MoS_2 film on SiO_2/Si (scale bar: 1 cm). (b) Raman spectra of the designated regions, which were labeled as 1−5 in panel a. (c) Mapping analysis of the numbered regions (1−5). The corresponding optical images are shown in the left column, Raman mappings of the intensity of A_{1g} in the middle column, and Raman mappings of peak position differences (Δ) between A_{1g} and E^1_{2g} in the right column (scale bar: 10 μm).

and electrical uniformity of all the devices on the SiO_2/Si chip, as-prepared thin films are required to be homogeneous over the entire substrate. In order to confirm the large-area uniformity of the MoS_2 film grown by our method, we sequentially selected five regions along the diagonal of the film (Figure 3a) and carried out morphology observation and structure analysis by Raman spectra, optical microscopy, and Raman and PL mappings (Figures 3b,c and S4). As shown in Figure 3b, representative Raman spectra at these regions were nearly identical, showing characteristic features of monolayer MoS_2 with a Δ value (peak position differences between A_{1g} and E^1_{2g}) of 19.2 cm^{-1}. Mapping results over the designated regions also confirmed the film was monolayer, where both distributions of intensities of A_{1g} mode and Δ value were highly uniform. In addition, PL spectra and mapping at these regions were also uniform in both peak position (a single peak of ~1.84 eV) and intensity (Figure S4), which was additional evidence of high-quality monolayer MoS_2. Corresponding optical images demonstrated that they were continuous at these locations. Therefore, considering the morphology observation and structure analysis, the as-grown MoS_2 films were continuous and uniform at the centimeter scale.

We next investigated the electrical uniformity of as-grown MoS_2 films by fabricating field effect transistor arrays. Compared to randomly distributed MoS_2 triangle domains which were normally achieved by the CVD method, the device fabrication process was dramatically simplified on as-obtained continuous MoS_2 film. Rather than using complicated and time-consuming EBL to define contact electrodes on selective MoS_2 domains, we simply patterned Cr/Au as top contact electrodes by photolithography with 300 nm SiO_2 as the dielectric layer and highly doped Si as the back gate (Figure S5a). Figure 4a is a photo of 8 × 8 MoS_2 FET arrays, where channel length (L) and width (W) were ~8.5 μm and ~50 μm, respectively, and yields of them were about 90%. Panels c and d of Figure 4 are representative output and transfer curves, showing a typical n-type behavior with an electron mobility of 0.88 $cm^2\ V^{-1}\ s^{-1}$ and on/off current ratio of $>10^6$. Carrier mobility can be calculated from the linear regime of the transfer characteristics.[32,38,39] Based on the statistics of 100 MoS_2 FETs, the mobility value fell in a range of 0.6−5.9 $cm^2\ V^{-1}\ s^{-1}$ with normal distribution. The average electron mobility of as-grown MoS_2 films was about 2.4 $cm^2\ V^{-1}\ s^{-1}$, and the maximum value can reach as high as 5.9 $cm^2\ V^{-1}\ s^{-1}$ (Figures 4d and S5b,c). The on/off ratio fell in the range of 1 × 10^5 to 1.6 × 10^6 (Figure S5d). These results confirmed that the as-grown MoS_2 film possessed spatial homogeneity in electrical performance over centimeter areas. Furthermore, the maximum mobility of as-obtained continuous monolayer MoS_2 film was comparable to those of samples grown by many methods,[15,24,25,29] suggesting that MoS_2 film synthesized in this work has great potential in large-area device fabrication.

We attribute the formation mechanism of high-quality and continuous MoS_2 film to the synergistic modulating of precursor and promoter. First, we compared electrochemically oxidized and nonoxidized Mo foil as precursors to grow MoS_2. As shown in Figure 5a, at the same growth conditions (temperature, growth time, carrier air, Na_2SO_4 additive, etc.),

https://dx.doi.org/10.1021/acs.jpclett.9b03879
J. Phys. Chem. Lett. 2020, 11, 1570−1577

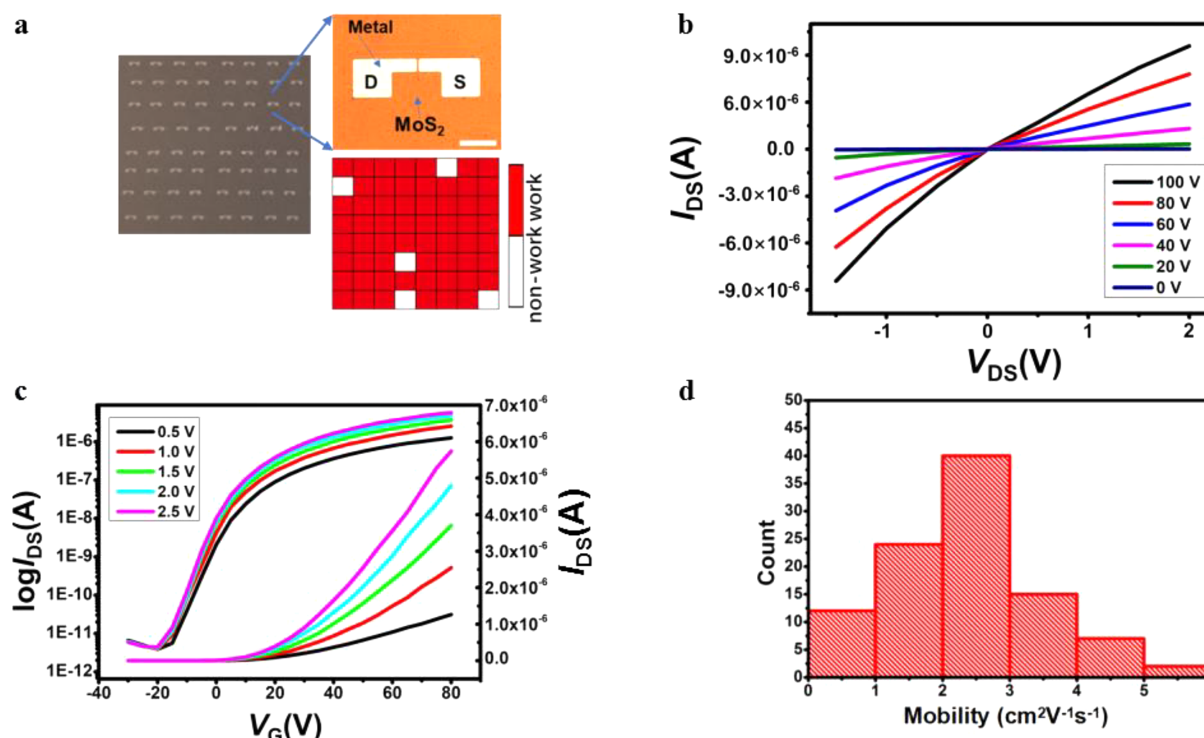

Figure 4. Electrical performance of uniform and continuous MoS_2 film. (a) Photo of 8 × 8 MoS_2 FET arrays fabricated on 1 × 1 cm^2 SiO_2/Si substrate. Top inset: a zoomed-in view of the optical image on an individual FET with channel length and width of 8.5 and 50 μm (scale bar: 100 μm). Bottom inset: corresponding success rate of FET arrays. Red and white represent working and nonworking devices, respectively. (b and c) Output (b) and transfer (c) characteristics for a typical MoS_2 FET. (d) Distribution of mobilities of 100 FETs.

using Mo foil as precursor we could obtain only randomly distributed MoS_2 domains. If there was no Na_2SO_4 additive, nothing would be grown by the Mo foil as precursor (Figure 5b). In contrast, MoO_x foil as precursor easily led to continuous MoS_2 film on SiO_2/Si (Figure 1i). The following chemical reactions can be used to understand this phenomenon:

$$2Mo + xO_2 \rightarrow 2MoO_x \quad (1)$$

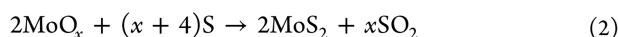

$$2MoO_x + (x + 4)S \rightarrow 2MoS_2 + xSO_2 \quad (2)$$

With Mo foil as precursor, an oxidized procedure with oxygen was required, which would decrease the reaction speed and increase the complexity of reaction systems.

Second, we conducted a series of theoretical calculations and experiments to understand the role of Na_2SO_4. Previous work has indicated that the introduction of alkali metal halides is helpful for the CVD growth of 2D materials. NaCl decreases the melting point of the reactants and facilitates the formation of intermediate products, increasing the overall reaction rate.[27−31] In this work, Na_2SO_4 was used as a synergistic additive instead of alkali metal halides such as NaCl and NaF. This is because the sulfate ion does not introduce heteroatoms into the system, and at high temperature, sulfate ions are decomposed into SO_2 gas, avoiding the contamination of as-grown MoS_2. For example, NaF as synergistic addictive would leave contamination on the surface of the MoS_2 film (Figure S6). In contrast, Na_2SO_4 as additive led to a clean surface of the MoS_2 film (Figure 1i).

We considered four Na-MoS_2/SiO_2 systems, including the Na atom adsorbed on the upper and lower surface of MoS_2, on the midperpendicular plane of the MoS_2/SiO_2 interface, and on the topmost layer of the SiO_2 (Figure 5d). The DFT-calculated total energies showed that the presence of Na atoms between monolayer MoS_2 and SiO_2 substrate led to a lower system energy compared with that of the adsorbed Na atoms on the upper surface of MoS_2. It was worth noting that whether the Na atom is close to MoS_2 or SiO_2 substrate, or at precisely the middle of MoS_2 and SiO_2, the most stable structure is that in which the Na atoms bonded with the O atoms of the SiO_2 substrate. In addition, only small-area MoS_2 could be grown on the Si substrate, indicating that SiO_2 was involved in the reaction (Figure 5c). The chemical reaction between Na and the system of monolayer MoS_2/SiO_2 should be the following:

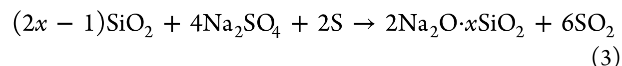

$$(2x - 1)SiO_2 + 4Na_2SO_4 + 2S \rightarrow 2Na_2O{\cdot}xSiO_2 + 6SO_2 \quad (3)$$

These all suggested that Na tended to bond with SiO_2 substrates rather than to interfere with as-grown MoS_2, which will result in high-quality MoS_2.

To elucidate that Na as a promoter solely interacted with SiO_2 substrate, XPS was performed to probe the bonding information on as-grown and transferred MoS_2 on SiO_2/Si (Figure 5e−g). For as-grown MoS_2 on SiO_2/Si, XPS spectra of Mo 3d, S 2s, and S 2p were consistent with the that reported in the literature for MoS_2 single crystal,[30] and the ratio of Mo to S is 1:2, further confirming the high quality of our MoS_2 film (Figures 5e and S7). XPS spectra of Na 2p, Na 2s, and Na 1s also indicated the formation of Na_2O (Figure 5f,g). After MoS_2 was transferred onto a second SiO_2/Si substrate, there was no Na signal any more (Figure 5f,g). Meanwhile, after transfer, on the as-grown SiO_2/Si substrate, the Na peak still existed without any MoS_2 trace (Figure S8). These results indicated that Na only reacted with SiO_2/Si substrate, and it does not

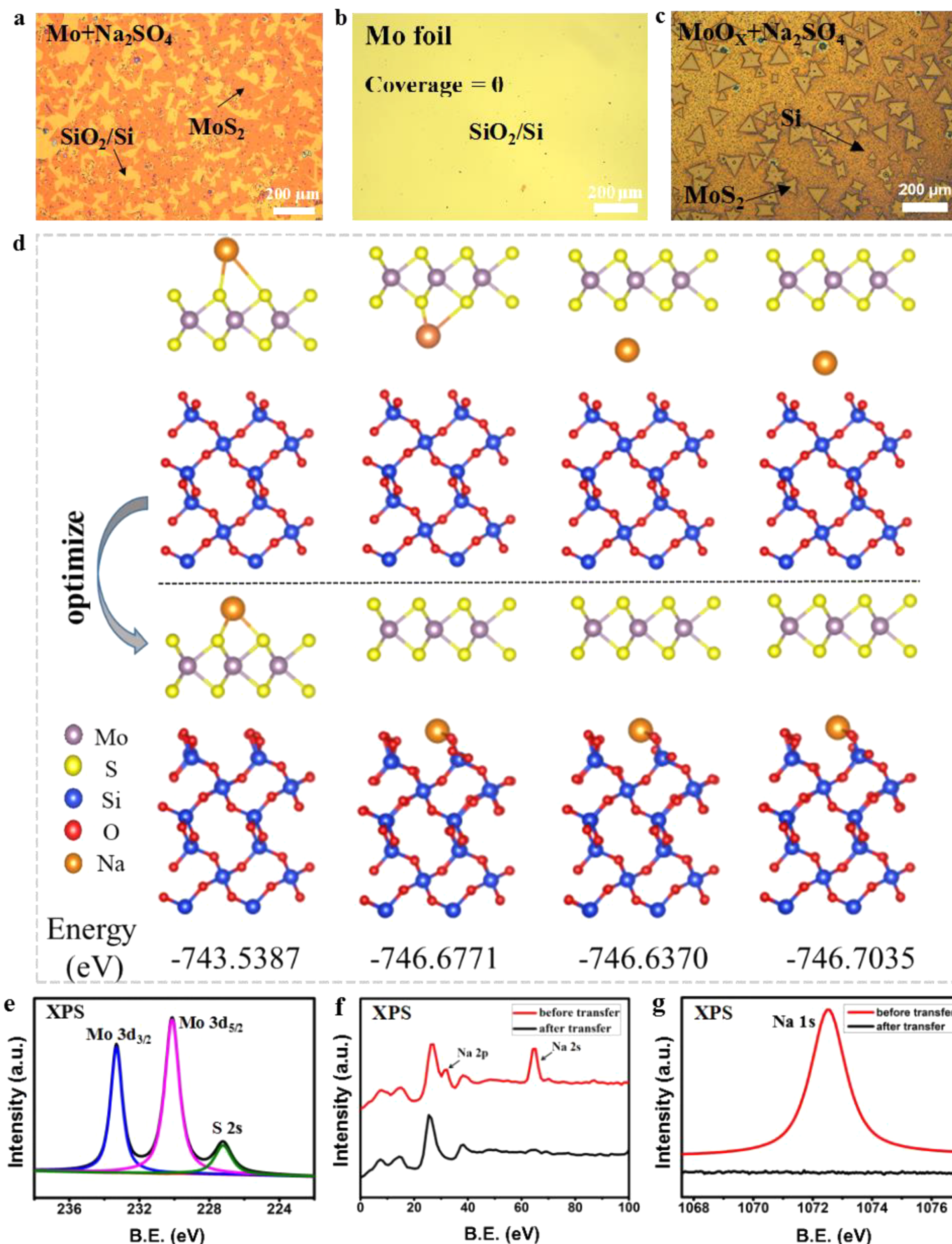

Figure 5. Synergistic growth mechanism of MoS_2. (a and b) Optical images of MoS_2 grown with Mo as precursor with (a, 0.05 mol/L) and without (b) Na_2SO_4 additive on SiO_2/Si substrate. (c) Optical image of MoS_2 grown with MoO_x as precursor with 0.05 mol/L Na_2SO_4 additive on Si substrate. (d) Original (top panel) and optimized (bottom panel) structures of monolayer MoS_2 on SiO_2 with an adsorbed Na atom. The corresponding total energy of each system is shown below the relaxed equilibrium geometry. (e) XPS data of Mo 3d, S 2s regions for MoS_2. (f and g) XPS data of Na 2p, Na 2s, and Na 1s for MoS_2 before and after transfer.

affect the growth quality of MoS_2, which had also been proved by TEM observations and electrical tests. Therefore, by synergistically tuning the Mo source and Na catalysis, continuous and high-quality MoS_2 film can be achieved on

https://dx.doi.org/10.1021/acs.jpclett.9b03879
J. Phys. Chem. Lett. 2020, 11, 1570−1577

SiO_2/Si substrates, pushing 2D materials one step closer to real applications.

In summary, we demonstrated large-area growth of uniform and continuous MoS_2 film on SiO_2/Si substrates by synergistically mediating both precursor and catalyst during the CVD process. As-grown MoS_2 films exhibited good crystallinity, high-quality, and homogeneity, showing domain sizes as large as 632 μm and electron mobilities as high as 5.9 $cm^2\ V^{-1}\ s^{-1}$. Face-to-face MoO_x foil as precursor and Na_2SO_4 as promoter played critical roles in this growth method, and they did not affect the final quality of the MoS_2 film. This methodology can be further extended to grow other layered TMDs, paving a new road toward large-area production of layered TMDs for both fundamental research and industrial applications.

■ ASSOCIATED CONTENT

Supporting Information

The Supporting Information is available free of charge at https://pubs.acs.org/doi/10.1021/acs.jpclett.9b03879.

> Experimental details and figures including optical images of as-grown MoS_2, PL mappings, electrical data, and XPS data (PDF)

■ AUTHOR INFORMATION

Corresponding Authors

Zhenquan Tan − *State Key Laboratory of Fine Chemicals, Panjin Branch of School of Chemical Engineering, Dalian University of Technology, Panjin 124221, Liaoning, China;* orcid.org/0000-0002-1730-7290; Email: tanzq@dlut.edu.cn

Xue-Zhi Song − *State Key Laboratory of Fine Chemicals, Panjin Branch of School of Chemical Engineering, Dalian University of Technology, Panjin 124221, Liaoning, China;* orcid.org/0000-0001-9574-1570; Email: songxz@dlut.edu.cn

Nan Liu − *Beijing Key Laboratory of Energy Conversion and Storage Materials, College of Chemistry, Beijing Normal University, Beijing 100875, China;* orcid.org/0000-0002-1793-7372; Email: nanliu@bnu.edu.cn

Authors

Guanmeng Li − *State Key Laboratory of Fine Chemicals, Panjin Branch of School of Chemical Engineering, Dalian University of Technology, Panjin 124221, Liaoning, China; Beijing Key Laboratory of Energy Conversion and Storage Materials, College of Chemistry, Beijing Normal University, Beijing 100875, China*

Xiaoli Wang − *College of Chemistry, Key Laboratory of Theoretical & Computational Photochemistry of Ministry of Education, Beijing Normal University, Beijing 100875, China*

Bo Han − *International Center for Quantum Materials and Electron Microscopy Laboratory, School of Physics, Peking University, Beijing 100871, China*

Weifeng Zhang − *Beijing Key Laboratory of Energy Conversion and Storage Materials, College of Chemistry, Beijing Normal University, Beijing 100875, China*

Shuyan Qi − *Beijing Key Laboratory of Energy Conversion and Storage Materials, College of Chemistry, Beijing Normal University, Beijing 100875, China*

Yan Zhang − *Beijing Key Laboratory of Energy Conversion and Storage Materials, College of Chemistry, Beijing Normal University, Beijing 100875, China*

Jiakang Qiu − *Beijing Key Laboratory of Energy Conversion and Storage Materials, College of Chemistry, Beijing Normal University, Beijing 100875, China*

Peng Gao − *International Center for Quantum Materials and Electron Microscopy Laboratory, School of Physics, Peking University, Beijing 100871, China; Collaborative Innovation Center of Quantum Matter, Beijing 100871, China;* orcid.org/0000-0003-0860-5525

Shaoshi Guo − *Beijing Key Laboratory of Energy Conversion and Storage Materials, College of Chemistry, Beijing Normal University, Beijing 100875, China*

Run Long − *College of Chemistry, Key Laboratory of Theoretical & Computational Photochemistry of Ministry of Education, Beijing Normal University, Beijing 100875, China;* orcid.org/0000-0003-3912-8899

Complete contact information is available at: https://pubs.acs.org/10.1021/acs.jpclett.9b03879

Notes

The authors declare no competing financial interest.

■ ACKNOWLEDGMENTS

N.L. acknowledges National Natural Science Foundation of China (21903007), Young Thousand Talents Program (110532103), Beijing Normal University Startup funding (312232102), and the Fundamental Research Funds for the Central Universities (310421109). We thank the analytical instrumentation center of Peking University for its technical support on XPS. We thank Mr. Zeshi Zhang (Dalian University of Technology) for his advice on the DFT calculation. We thank Electron Microscopy Laboratory at Peking University for the use of Cs corrected electron microscope.

■ REFERENCES

(1) Radisavljevic, B.; Radenovic, A.; Brivio, J.; Giacometti, V.; Kis, A. Single-Layer MoS_2 Transistors. *Nat. Nanotechnol.* **2011**, *6*, 147−150.

(2) Liu, L.; Wu, J.; Wu, L.; Ye, M.; Liu, X.; Wang, Q.; Hou, S.; Lu, P.; Sun, L.; Zheng, J.; Xing, L.; Gu, L.; Jiang, X.; Xie, L.; Jiao, L. Phase-Selective Synthesis of 1T' MoS_2 Monolayers and Heterophase Bilayers. *Nat. Mater.* **2018**, *17*, 1108−1114.

(3) Zeng, M.; Xiao, Y.; Liu, J.; Yang, K.; Fu, L. Exploring Two-Dimensional Materials toward the Next-Generation Circuits: From Monomer Design to Assembly Control. *Chem. Rev.* **2018**, *118*, 6236−6296.

(4) Sun, L.; Yan, X.; Zheng, J.; Yu, H.; Lu, Z.; Gao, S. P.; Liu, L.; Pan, X.; Wang, D.; Wang, Z.; Wang, P.; Jiao, L. Layer-Dependent Chemically Induced Phase Transition of Two-Dimensional MoS_2. *Nano Lett.* **2018**, *18*, 3435−3440.

(5) Dankert, A.; Pashaei, P.; Kamalakar, M. V.; Gaur, A. P. S.; Sahoo, S.; Rungger, I.; Narayan, A.; Dolui, K.; Hoque, M. A.; Patel, R. S.; de Jong, M. P.; Katiyar, R. S.; Sanvito, S.; Dash, S. P. Spin-Polarized Tunneling through Chemical Vapor Deposited Multilayer Molybdenum Disulfide. *ACS Nano* **2017**, *11*, 6389−6395.

(6) Kim, S.; Konar, A.; Hwang, W. S.; Lee, J. H.; Lee, J.; Yang, J.; Jung, C.; Kim, H.; Yoo, J. B.; Choi, J. Y.; Jin, Y. W.; Lee, S. Y.; Jena, D.; Choi, W.; Kim, K. High-Mobility and Low-Power Thin-Film Transistors Based on Multilayer MoS_2 Crystals. *Nat. Commun.* **2012**, *3*, 1011.

(7) Chen, S.; Gao, J; Srinivasan, B. M.; Zhang, Y.-W. A Kinetic Monte Carlo Study for Mono- and Bi-layer Growth of MoS_2 during Chemical Vapor Deposition. *Acta Physico-Chimica Sinica* **2019**, *35*, 1119−1127.

(8) Desai, S. B.; Madhvapathy, S. R.; Sachid, A. B.; Llinas, J. P.; Wang, Q.; Ahn, G. H.; Pitner, G.; Kim, M. J.; Bokor, J.; Hu, C. MoS_2 transistors with 1-nanometer gate lengths. *Science* **2016**, *354*, 99−102.
(9) Chee, S. S.; Seo, D.; Kim, H.; Jang, H.; Lee, S.; Moon, S. P.; Lee, K. H.; Kim, S. W.; Choi, H.; Ham, M. H. Lowering the Schottky Barrier Height by Graphene/Ag Electrodes for High-Mobility MoS_2 Field-Effect Transistors. *Adv. Mater.* **2019**, *31*, No. 1804422.
(10) Lopez-Sanchez, O.; Lembke, D.; Kayci, M.; Radenovic, A.; Kis, A. Ultrasensitive Photodetectors Based on Monolayer MoS_2. *Nat. Nanotechnol.* **2013**, *8*, 497−501.
(11) Lim, Y. R.; Song, W.; Han, J. K.; Lee, Y. B.; Kim, S. J.; Myung, S.; Lee, S. S.; An, K. S.; Choi, C. J.; Lim, J. Wafer-Scale, Homogeneous MoS_2 Layers on Plastic Substrates for Flexible Visible-Light Photodetectors. *Adv. Mater.* **2016**, *28*, 5025−5030.
(12) Zhu, H.; Wang, Y.; Xiao, J.; Liu, M.; Xiong, S.; Wong, Z. J.; Ye, Z.; Ye, Y.; Yin, X.; Zhang, X. Observation of Piezoelectricity in Free-Standing Monolayer MoS_2. *Nat. Nanotechnol.* **2015**, *10*, 151−155.
(13) Cai, Z.; Liu, B.; Zou, X.; Cheng, H. M. Chemical Vapor Deposition Growth and Applications of Two-Dimensional Materials and Their Heterostructures. *Chem. Rev.* **2018**, *118*, 6091−6133.
(14) Li, H.; Li, Y.; Aljarb, A.; Shi, Y.; Li, L. J. Epitaxial Growth of Two-Dimensional Layered Transition-Metal Dichalcogenides: Growth Mechanism, Controllability, and Scalability. *Chem. Rev.* **2018**, *118*, 6134−6150.
(15) Yang, P.; Zou, X.; Zhang, Z.; Hong, M.; Shi, J.; Chen, S.; Shu, J.; Zhao, L.; Jiang, S.; Zhou, X.; Huan, Y.; Xie, C.; Gao, P.; Chen, Q.; Zhang, Q.; Liu, Z.; Zhang, Y. Batch Production of 6-Inch Uniform Monolayer Molybdenum Disulfide Catalyzed by Sodium in Glass. *Nat. Commun.* **2018**, *9*, 979.
(16) Samadi, M.; Sarikhani, N.; Zirak, M.; Zhang, H.; Zhang, H.-L.; Moshfegh, A. Z. Group 6 Transition Metal Dichalcogenide Nanomaterials: Synthesis, Applications and Future Perspectives. *Nanoscale Horizons* **2018**, *3*, 90−204.
(17) Zhang, J.; Yu, H.; Chen, W.; Tian, X.; Liu, D.; Cheng, M.; Xie, G.; Yang, W.; Yang, R.; Bai, X.; Shi, D.; Zhang, G. Scalable Growth of High-Quality Polycrystalline MoS_2 Monolayers on SiO_2 with Tunable Grain Sizes. *ACS Nano* **2014**, *8*, 6024−6030.
(18) Kang, K.; Xie, S.; Huang, L.; Han, Y.; Huang, P. Y.; Mak, K. F.; Kim, C. J.; Muller, D.; Park, J. High-Mobility Three-Atom-Thick Semiconducting Films with Wafer-Scale Homogeneity. *Nature* **2015**, *520*, 656−660.
(19) Kim, H.; Ovchinnikov, D.; Deiana, D.; Unuchek, D.; Kis, A. Suppressing Nucleation in Metal-Organic Chemical Vapor Deposition of MoS_2 Monolayers by Alkali Metal Halides. *Nano Lett.* **2017**, *17*, 5056−5063.
(20) Boandoh, S.; Choi, S. H.; Park, J. H.; Park, S. Y.; Bang, S.; Jeong, M. S.; Lee, J. S.; Kim, H. J.; Yang, W.; Choi, J. Y.; Kim, S. M.; Kim, K. K. A Novel and Facile Route to Synthesize Atomic-Layered MoS_2 Film for Large-Area Electronics. *Small* **2017**, *13*, 1701306.
(21) Serna, M. I.; Yoo, S. H.; Moreno, S.; Xi, Y.; Oviedo, J. P.; Choi, H.; Alshareef, H. N.; Kim, M. J.; Minary-Jolandan, M.; Quevedo-Lopez, M. A. Large-Area Deposition of MoS_2 by Pulsed Laser Deposition with in Situ Thickness Control. *ACS Nano* **2016**, *10*, 6054−6061.
(22) Samassekou, H.; Alkabsh, A.; Wasala, M.; Eaton, M.; Walber, A.; Walker, A.; Pitkänen, O.; Kordas, K.; Talapatra, S.; Jayasekera, T.; Mazumdar, D. Viable Route Towards Large-Area 2D MoS^2 Using Magnetron Sputtering. *2D Mater.* **2017**, *4*, No. 021002.
(23) Jurca, T.; Moody, M. J.; Henning, A.; Emery, J. D.; Wang, B.; Tan, J. M.; Lohr, T. L.; Lauhon, L. J.; Marks, T. J. Low-Temperature Atomic Layer Deposition of MoS_2 Films. *Angew. Chem., Int. Ed.* **2017**, *56*, 4991−4995.
(24) Lin, Y. C.; Zhang, W.; Huang, J. K.; Liu, K. K.; Lee, Y. H.; Liang, C. T.; Chu, C. W.; Li, L. J. Wafer-Scale MoS_2 Thin Layers Prepared by MoO_3 Sulfurization. *Nanoscale* **2012**, *4*, 6637−6641.
(25) Liu, K. K.; Zhang, W.; Lee, Y. H.; Lin, Y. C.; Chang, M. T.; Su, C. Y.; Chang, C. S.; Li, H.; Shi, Y.; Zhang, H.; Lai, C. S.; Li, L. J. Growth of Large-Area and Highly Crystalline MoS_2 Thin Layers on Insulating Substrates. *Nano Lett.* **2012**, *12*, 1538−1544.
(26) Chen, T.; Zhou, Y.; Sheng, Y.; Wang, X.; Zhou, S.; Warner, J. H. Hydrogen-Assisted Growth of Large-Area Continuous Films of MoS_2 on Monolayer Graphene. *ACS Appl. Mater. Interfaces* **2018**, *10*, 7304−7314.
(27) Jiang, J.; Li, N.; Zou, J.; Zhou, X.; Eda, G.; Zhang, Q.; Zhang, H.; Li, L. J.; Zhai, T.; Wee, A. T. S. Synergistic Additive-Mediated Cvd Growth and Chemical Modification of 2D Materials. *Chem. Soc. Rev.* **2019**, *48*, 4639−4654.
(28) Zhou, J.; Lin, J.; Huang, X.; Zhou, Y.; Chen, Y.; Xia, J.; Wang, H.; Xie, Y.; Yu, H.; Lei, J.; Wu, D.; Liu, F.; Fu, Q.; Zeng, Q.; Hsu, C. H.; Yang, C.; Lu, L.; Yu, T.; Shen, Z.; Lin, H.; Yakobson, B. I.; Liu, Q.; Suenaga, K.; Liu, G.; Liu, Z. A Library of Atomically Thin Metal Chalcogenides. *Nature* **2018**, *556*, 355−359.
(29) Zhang, K.; Bersch, B. M.; Zhang, F.; Briggs, N. C.; Subramanian, S.; Xu, K.; Chubarov, M.; Wang, K.; Lerach, J. O.; Redwing, J. M.; Fullerton-Shirey, S. K.; Terrones, M.; Robinson, J. A. Considerations for Utilizing Sodium Chloride in Epitaxial Molybdenum Disulfide. *ACS Appl. Mater. Interfaces* **2018**, *10*, 40831−40837.
(30) Wang, P.; Lei, J.; Qu, J.; Cao, S.; Jiang, H.; He, M.; Shi, H.; Sun, X.; Gao, B.; Liu, W. Mechanism of Alkali Metal Compound-Promoted Growth of Monolayer MoS_2: Eutectic Intermediates. *Chem. Mater.* **2019**, *31*, 873−880.
(31) Hu, X.; Huang, P.; Liu, K.; Jin, B.; Zhang, X.; Zhang, X.; Zhou, X.; Zhai, T. Salt-Assisted Growth of Ultrathin Gese Rectangular Flakes for Phototransistors with Ultrahigh Responsivity. *ACS Appl. Mater. Interfaces* **2019**, *11*, 23353−23360.
(32) Zhu, J.; Xu, H.; Zou, G.; Zhang, W.; Chai, R.; Choi, J.; Wu, J.; Liu, H.; Shen, G.; Fan, H. MoS_2-OH Bilayer-Mediated Growth of Inch-Sized Monolayer MoS_2 on Arbitrary Substrates. *J. Am. Chem. Soc.* **2019**, *141*, 5392−5401.
(33) Liu, C.; Xu, X.; Qiu, L.; Wu, M.; Qiao, R.; Wang, L.; Wang, J.; Niu, J.; Liang, J.; Zhou, X.; Zhang, Z.; Peng, M.; Gao, P.; Wang, W.; Bai, X.; Ma, D.; Jiang, Y.; Wu, X.; Yu, D.; Wang, E.; Xiong, J.; Ding, F.; Liu, K. Kinetic Modulation of Graphene Growth by Fluorine through Spatially Confined Decomposition of Metal Fluorides. *Nat. Chem.* **2019**, *11*, 730−736.
(34) Yang, P.; Yang, A.-G.; Chen, L.; Chen, J.; Zhang, Y.; Wang, H.; Hu, L.; Zhang, R.-J.; Liu, R.; Qu, X.-P.; Qiu, Z.-J.; Cong, C. Influence of Seeding Promoters on the Properties of CVD Grown Monolayer Molybdenum Disulfide. *Nano Res.* **2019**, *12*, 823−827.
(35) Li, S.; Lin, Y. C.; Zhao, W.; Wu, J.; Wang, Z.; Hu, Z.; Shen, Y.; Tang, D. M.; Wang, J.; Zhang, Q.; Zhu, H.; Chu, L.; Zhao, W.; Liu, C.; Sun, Z.; Taniguchi, T.; Osada, M.; Chen, W.; Xu, Q. H.; Wee, A. T. S.; Suenaga, K.; Ding, F.; Eda, G. Vapour-Liquid-Solid Growth of Monolayer MoS_2 Nanoribbons. *Nat. Mater.* **2018**, *17*, 535−542.
(36) Chen, J.; Zhao, X.; Tan, S. J. R.; Xu, H.; Wu, B.; Liu, B.; Fu, D.; Fu, W.; Geng, D.; Liu, Y.; Liu, W.; Tang, W.; Li, L.; Zhou, W.; Sum, T. C.; Loh, K. P. Chemical Vapor Deposition of Large-Size Monolayer $MoSe_2$ Crystals on Molten Glass. *J. Am. Chem. Soc.* **2017**, *139*, 1073−1076.
(37) Lee, J. U.; Kim, K.; Han, S.; Ryu, G. H.; Lee, Z.; Cheong, H. Raman Signatures of Polytypism in Molybdenum Disulfide. *ACS Nano* **2016**, *10*, 1948−1953.
(38) Allain, A.; Kang, J.; Banerjee, K.; Kis, A. Electrical Contacts to Two-Dimensional Semiconductors. *Nat. Mater.* **2015**, *14*, 1195−1205.
(39) Liu, Y.; Guo, J.; Zhu, E.; Liao, L.; Lee, S. J.; Ding, M.; Shakir, I.; Gambin, V.; Huang, Y.; Duan, X. Approaching the Schottky-Mott Limit in Van Der Waals Metal-Semiconductor Junctions. *Nature* **2018**, *557*, 696−700.